Indian Journal of Pure & Applied Physics
Vol. 52, May 2014, pp. 314-321

Comprehensive study on energy absorption build-up factors and exposure build-up factors of solid state nuclear track detectors

Vishwanath P Singh[a]*, N M Badiger[a] & M E Medhat[b,c]

[a]Department of Physics, Karnatak University, Dharwad 580 003, India

[b]Experimental Nuclear Physics Department, Nuclear Research Centre, P.O. 13759, Cairo, Egypt

[c]Institute of High Energy Physics, CAS, Beijing 100 049, China

*E-mail: kudphyvps@rediffmail.com

Received 11 July 2013; revised 30 September 2013; accepted 9 January 2014

The gamma-ray build-up factors of solid state nuclear track detectors (SSNTDs) have been computed for photon energy in the range 0.015-15 MeV up to 40 mfp penetration depth by geometrical progression (GP) method. Significant variations in energy absorption build-up factors (EABFs) and exposure build-up factors (EBFs) for the investigated SSNTDs are observed. The EABFs and EBFs of the SSNTDs are strongly dependent upon the photon energy, penetration depths and the chemical compositions. The build-up factors are small in low and high photon energy whereas very large in medium energy region. The result could be useful in the field of radiation dosimetry of solid state nuclear track detectors for gamma dose measurements.

Keywords: Exposure, Energy absorption, GP fitting, Gamma, Solid state nuclear track detectors, Radiation dosimetry

1 Introduction

Solid state nuclear track detectors (SSNTDs) have potential applications in diverse areas such as nuclear dosimeters, nuclear technology, astrophysics, material sciences and environmental science. There are several types of detectors which include photographic emulsion, inorganic crystals, glasses, plastics and minerals. SSNTDs are capable to detect ions, fission fragments, charged particles, neutrons and photons. The SSNTDs provide quantitative and qualitative analysis of particles regarding to their charge, mass, direction of motion as well as energy. SSNTDs are used for detection of neutrons of different energies like thermal, epithermal, intermediate, fast and very fast energies. SSNTDs are utilized for estimation of uranium concentrations, building materials and internal contamination of radon in dwellings and personnel dosimetry[1,2].

CR-39 is being used for particle induced nuclear reactions[3-7] spontaneous fission measurement[8,9], heavy ion interactions, dating of micro-craters, formed on the lunar surface, fission track dating of bio-titer mica from Antarctica[10,11], evolution of an Am–Be neutron source, high gamma dose measurements[12,13] registration of the tracks of anti-proton and study of the annihilation of anti-proton, radon measurement[14-16] and neutron dosimetry. CR-39 is sensitive track detector which is being used for fast personnel neutron dosimetry for energy ranging from 100 keV to 20 MeV. CR-39 is being used for personnel monitoring in nuclear reactors (8-10 MeV) and accelerators of average neutron energy in the range 0.82-11.6 MeV and neutron of energy 1.5 MeV in proton accelerator[17-20].

The SSNTDs are used in neutron, gamma and mixture of neutron and gamma radiation field. The irradiation with gamma rays may lead to significant effects on the properties of track detectors. Plastic SSNTDs have been utilized for gamma dose measurement earlier [21]. Makrofol-N, LR-115, CR-39, Marofol-E, Daicel, CA80-15, and CN-85 plastic track detectors are calibrated in the gamma dose in the range 10^3-10^6 Gy for ^{60}Co source and gamma radiations have been measured for fuel element[13].

The interaction of gamma rays with SSNTDs may affect the tracks registrations as well internal structure of the detector[22-25]. Gamma rays measurement requires accurate knowledge of energy loss in the detector medium by absorption build-up factors and exposure build-up factors. The build-up factors for gamma photon may possibly explore the explanation of track formation and sensitivities of SSNTDs for gamma radiation measurement as well as interferences of gamma with neutron measurement. This motivated us for investigation of energy absorption and exposure build-up factors for gamma rays in these SSNTD materials.

The compilation for build-up factors by various codes is reported in ANSI/ANS-6.4.3 by American Nuclear Society[26]. The data in the report covers energy in the range 0.015-15 MeV up to penetration depth of 40 mean free path (mfp). The build-up factors in the ANS-6.4.3 are for 23 elements of atomic number, $Z = 4$ to 92. The build-up factors of ANS-6.4.3 can also be calculated by invariant embedding[27]. Harima *et al*[28]. developed a fitting formula, called Geometrical Progression (GP) which gives build-up factors of the good agreement with ANS-6.4.3. The GP fitting formula is known to be accurate within the estimated uncertainty (<5%). Harima[29] reviewed historical and reported the current gamma photon build-up factors. Various researchers investigated gamma ray build-up factors in different materials; silicate, neutron shielding, concretes, human teeth and thermoluminescent dosimetric[30-35] which shows that the GP fitting is very useful and accurate method for estimation of exposure and energy absorption build-up factors.

The exposure build-up factors (EBFs) and energy absorption build-up factors (EABFs) of the SSNTDs were computed for the first time by GP fitting formula in the photon energy range 0.015-15 MeV up to 40 mfp. We also discussed dependency of EBF on photon energy, penetration depth and chemical compositions of the SSNTDs. This study should be useful for track registrations, damages and other gamma interaction properties of SSNTDs.

2 Materials and Methods

The elemental compositions of the SSNTDs is given in Table 1. These neutron detectors are commonly used for measurement of neutorn and gamma radiation.

2.1 Computational Method

The exposure build-up factors (EBFs), energy absorption build-up factors (EABFs) and GP fitting parameters are calculated by method of interpolation from the equivalent atomic number (Z_{eq}) of the SSNTD materials. The computational work of these parameters is done in three steps as:

(1) Calculation of equivalent atomic number, Z_{eq}
(2) Calculation of G-P fitting parameters
(3) Calculation of build-up factors

Z_{eq} is a parameter which describes the composite SSNTD material properties in terms of equivalent elements similar to atomic number for a single element. Since interaction processes of gamma ray with matter, photo-electric absorption, Compton scattering and pair-production are energy dependent therefore, Z_{eq} for each interaction varies according to the photon energy. However. the build-up of photons is mainly due to multiple scattering events by Compton scattering, so that Z_{eq} is derived from the Compton scattering interaction process.

The Z_{eq} for a SSNTD is estimated by matching the ratio of $(\mu/\rho)_{Compton}/(\mu/\rho)_{Total}$, of that detector at a specific energy with the corresponding ratio of an element at the same energy. Thus, firstly the Compton partial mass attenuation coefficient, $(\mu/\rho)_{Compton}$ and the total mass attenuation coefficients, $(\mu/\rho)_{Total}$, were obtained for elements Z= 1 to 30 and for the chosen SSNTD in the energy region 0.015-15 MeV using WinXCom computer program[36,37] initially developed as XCOM[38]. For the interpolation of Z_{eq} for which the ratio $(\mu/\rho)_{Compton}/(\mu/\rho)_{Total}$ lies between two successive ratios of elements, the following formula was employed[39,40]:

$$Z_{eq} = \frac{Z_1(\log R_2 - \log R) + Z_2(\log R - \log R_1)}{\log R_2 - \log R_1} \quad \ldots(1)$$

where Z_1 and Z_2 are the atomic numbers of elements corresponding to the ratios R_1 and R_2 respectively, R is the ratio for the chosen SSNTD at a specific energy. The calculated Z_{eq} of the SSNTDs are given in Table 2.

Table 1—Elemental compositions of Solid State Nuclear Track detectors[23]

Sr. No.	SSNTD type	Elemental composition (%)
1	Apatite	H: 0.07; O: 39.19; F: 0.13;P: 18.46;Cl: 2.35;Ca: 39.80
2	Diopside	O: 44.330; Mg: 11.22; Si: 25.940; Ca: 18.51
3	Merrillite	H: 0.09; O: 41.81; Mg: 1.59; P: 20.24; Ca: 33.66; Fe: 2.61
4	Phlogopite	H: 0.24; O: 41.98; F: 4.53; Mg: 17.39; Al: 6.44; Si: 20.09; K: 9.33
5	Oligoclase	O: 48.22 ; Na: 6.93; Al: 12.20; Si: 29.63; Ca: 3.02
6	Titanite	O: 48.81; Si: 14.33;Ca: 20.44; Ti: 24.42
7	Glass Phosphate	O: 42.28; Na: 2.95;Al: 2.65; P: 24.00; Zn: 28.12
8	CR39	H: 6.62; C: 52.55; O: 40.83

Table 2 — Equivalent atomic numbers of the Solid State Nuclear Track Detectors

Energy (meV)	Apatite	Diopside	Merrillite	Phlogopite	Oligoclase	Titanite	Glass Phosphate	CR39
0.015	15.745	13.584	15.603	12.221	11.785	16.381	19.120	6.744
0.02	15.887	13.706	15.765	12.303	11.846	16.563	19.476	6.758
0.03	16.026	13.830	15.926	12.391	11.917	16.739	19.888	6.769
0.04	16.115	13.913	16.027	12.446	11.965	16.846	20.127	6.776
0.05	16.178	13.974	16.103	12.483	12.001	16.926	20.315	6.781
0.06	16.226	14.020	16.161	12.510	12.027	16.987	20.455	6.786
0.08	16.283	14.079	16.231	12.548	12.059	17.069	20.656	6.792
0.1	16.322	14.119	16.280	12.575	12.082	17.121	20.791	6.797
0.15	16.379	14.179	16.351	12.617	12.113	17.195	21.002	6.805
0.2	16.412	14.215	16.393	12.642	12.132	17.238	21.122	6.805
0.3	16.450	14.253	16.441	12.674	12.156	17.287	21.255	6.811
0.4	16.471	14.275	16.467	12.691	12.167	17.314	21.331	6.813
0.5	16.483	14.288	16.482	12.699	12.171	17.329	21.374	6.814
0.6	16.489	14.294	16.491	12.703	12.175	17.338	21.402	6.815
0.8	16.496	14.300	16.500	12.707	12.180	17.347	21.429	6.815
1	16.495	14.300	16.499	12.708	12.179	17.346	21.430	6.815
1.5	15.068	12.795	14.908	11.571	11.214	15.649	18.683	6.187
2	14.520	12.387	14.236	11.323	11.019	14.935	16.738	6.162
3	14.330	12.274	14.021	11.266	10.976	14.684	16.049	6.156
4	14.289	12.234	13.978	11.241	10.953	14.625	15.887	6.153
5	14.263	12.230	13.947	11.234	10.946	14.594	15.814	6.152
6	14.249	12.218	13.934	11.232	10.946	14.576	15.767	6.151
8	14.239	12.210	13.921	11.223	10.938	14.561	15.714	6.148
10	14.228	12.204	13.909	11.220	10.934	14.547	15.686	6.146
15	14.217	12.196	13.897	11.217	10.933	14.537	15.659	6.145

The GP fitting parameters were calculated in a similar fashion of interpolation procedure for Z_{eq}. The GP fitting parameters for the elements were taken from the ANS-6.4.3 standard reference database which provides the GP fitting parameters for twenty three elements (beryllium, Z=4 to iron, Z=26) in the energy region 0.015-15 MeV up to 40 mfp penetration depth. The G-P fitting parameters for the SSNTD materials were interpolated by:

$$C = \frac{C_1(\log Z_2 - \log Z_{eq}) + C_2(\log Z_{eq} - \log Z_1)}{\log Z_2 - \log Z_1} \quad \ldots (2)$$

where C_1 and C_2 are the values of the GP fitting parameters corresponding to the atomic numbers of Z_1 and Z_2, respectively.

Third and final step is build-up factors estimation by GP fitting parameters (b, c, a, X_k and d) in the photon energy range 0.015-15 MeV up to a 40 mfp by equations Harima *et al*[28]. as:

$$B(E,x) = 1 + \frac{(b-1)(K^x - 1)}{K - 1} \quad \text{for} \quad K \neq 1 \quad \ldots (3)$$

$$B(E,x) = 1 + (b-1)x \quad \text{for} \quad K = 1 \quad \ldots (4)$$

where

$$K(E,x) = cx^a + d\frac{\tanh(x/X_K - 2) - \tanh(-2)}{1 - \tanh(-2)}$$

For penetration depth (X)≤40 mfp …(5)

where x is the source-detector distance for the medium in terms of mfp and b, the value of the exposure build-up factor at 1 mfp, K (E, X) is the dose multiplicative factor, and b, c, a, X_K and d are computed GP fitting parameters which depend on the attenuating medium and source energy. The GP fitting parameters of EABF and EBF of CR-39 are given in Table 3. Similarly, the GP parameters of remaining SSNTDs can be calculated.

3 Uncertainty in Calculation

The uncertainties in the build-up factor by GP fitting[26,41] are comparable with ANS-6.4.3 standard and MCNP-5 for air and water. The build-up factors by ANSI-6.4.3, GP fitting formulae and MCNP-5 for EBF of water have been compared for photon energy[32] range 0.015-15 MeV up to 40 mfp. The MCNP-5 results vary from those ANS-6.4.3 standards with

Table 3 — GP fitting parameters of CR-39 SSNTD

Energy (MeV)	CR-39									
	EBF					EABF				
	b	*c*	*a*	Xk	*d*	*b*	*c*	*a*	Xk	*D*
1.50E-02	1.271	0.490	0.165	14.280	–0.082	1.275	0.495	0.161	14.534	–0.078
2.00E-02	1.619	0.619	0.118	15.358	–0.058	1.637	0.615	0.121	15.255	–0.059
3.00E-02	2.814	0.910	0.036	15.082	–0.029	2.932	0.910	0.035	15.294	–0.027
4.00E-02	4.222	1.377	–0.069	13.650	0.027	4.212	1.370	–0.067	13.863	0.015
5.00E-02	5.383	1.736	–0.125	13.951	0.054	5.038	1.720	–0.122	14.067	0.049
6.00E-02	5.853	2.027	–0.163	13.852	0.075	5.201	1.993	–0.158	13.950	0.069
8.00E-02	5.780	2.363	–0.200	13.523	0.091	5.013	2.276	–0.190	13.700	0.082
1.00E-01	5.505	2.409	–0.200	14.392	0.087	4.699	2.305	–0.188	14.556	0.078
1.50E-01	4.045	2.529	–0.216	14.116	0.097	3.708	2.334	–0.192	14.511	0.078
2.00E-01	3.460	2.461	–0.213	13.643	0.092	3.330	2.226	–0.182	14.794	0.077
3.00E-01	2.995	2.190	–0.185	14.122	0.079	2.833	2.069	–0.169	14.343	0.068
4.00E-01	2.725	2.015	–0.168	13.948	0.071	2.622	1.903	–0.151	14.321	0.062
5.00E-01	2.559	1.866	–0.150	14.140	0.064	2.461	1.788	–0.138	14.457	0.057
6.00E-01	2.430	1.757	–0.137	14.021	0.058	2.369	1.677	–0.123	14.369	0.052
8.00E-01	2.253	1.599	–0.116	13.990	0.051	2.201	1.547	–0.106	14.181	0.044
1.00E+00	2.151	1.486	–0.098	13.937	0.044	2.104	1.435	–0.087	14.630	0.037
1.50E+00	2.002	1.303	–0.067	13.913	0.031	1.939	1.275	–0.060	14.308	0.038
2.00E+00	1.891	1.189	–0.043	13.983	0.020	1.842	1.169	–0.038	14.430	0.025
3.00E+00	1.746	1.059	–0.014	12.309	0.006	1.714	1.051	–0.011	14.183	0.013
4.00E+00	1.649	0.986	0.004	24.011	–0.007	1.626	0.988	0.004	13.065	0.001
5.00E+00	1.573	0.939	0.017	14.351	–0.011	1.564	0.944	0.015	14.800	–0.004
6.00E+00	1.524	0.907	0.027	14.054	–0.015	1.515	0.906	0.028	13.121	–0.008
8.00E+00	1.437	0.871	0.037	16.226	–0.032	1.430	0.882	0.034	12.099	–0.019
1.00E+01	1.371	0.858	0.041	12.640	–0.021	1.376	0.861	0.040	14.322	–0.017
1.50E+01	1.275	0.841	0.046	15.234	–0.030	1.281	0.838	0.047	15.769	–0.033

greatest 13.83% due to difference in cross-section libraries, method of solution for codes, calculation methods, standard deviation and physics assumptions for Bremsstrahlung and coherent scattering[41]. It is reported that the invariant embedding, GP fitting and MCNP simulation are in good agreement for low-Z materials (Z<18) with small discrepancies[27]. The comparison between the absolute values of the maximum deviations in the Berger fitting[42], Taylor fitting[43], three-exponential[44] and GP fitting of the EBFs in water up to 40 mfp in thickness is shown in Fig. 1. The most reliable and accurate formula is the GP fitting method. The absolute maximum deviation in EBF by GP fitting is 0.5-3%, 0.9-42.7% for Berger approach, 0.4-53.2% for Taylor approach and 0.5-9.3% for three-exponential methods[29].

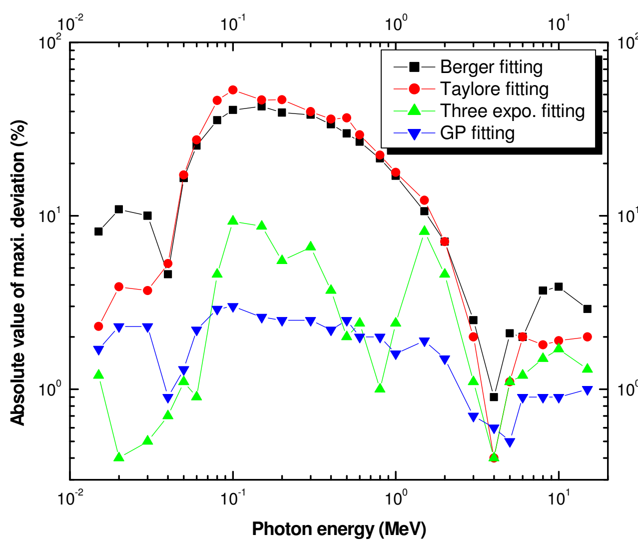

Fig. 1 — Comparison of absolute value of maximum deviation of build-up factors by (i) Berger fitting (ii) Taylor fitting (iii) Three exponential fitting and (iv) GP fitting

4 Results and Discussion

Gamma ray energy absorption build-up factors (EABFs) and exposure build-up factors (EBFs) of solid state neutron track detectors have been computed. The EABFs and EBFs for photon energy in the range 0.015-15 MeV up to 40 mfp penetration depth are shown in Figs 2(a-e) and 3(a-e) at penetration depths 1, 5, 10, 20 and 40 mfps. The variations of EABFs and EBFs of the neutron detector have been explained for dependency upon photon energy, penetration depths of dosimeters and chemical compositions of the dosimeters in detail.

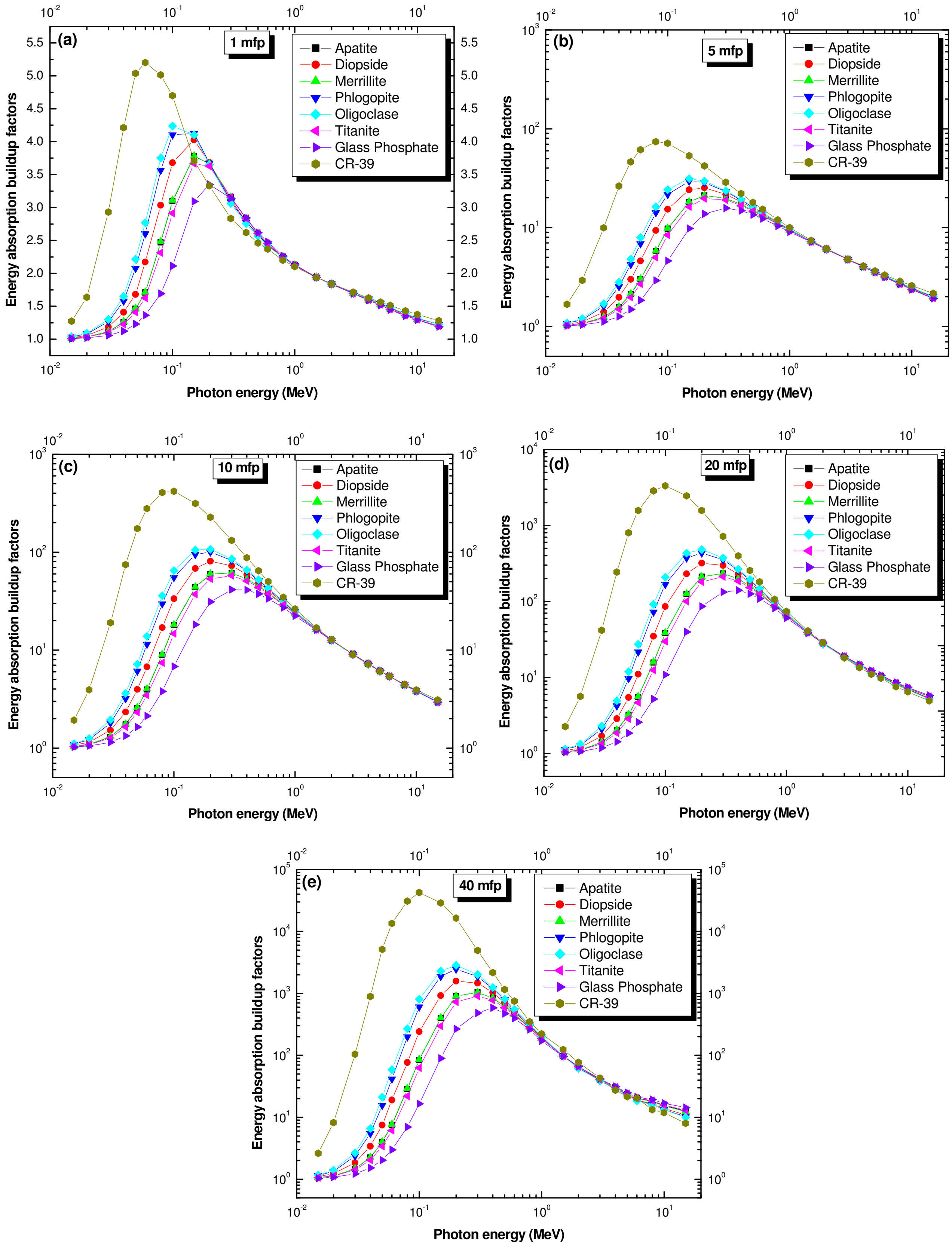

Fig. 2 — Energy absorption buildup factors of solid state neutron tract detectors (a) 1 mfp (b) 5 mfp (c) 10 mfp (d) 20 mfp and (e) 40 mfp penetration depths

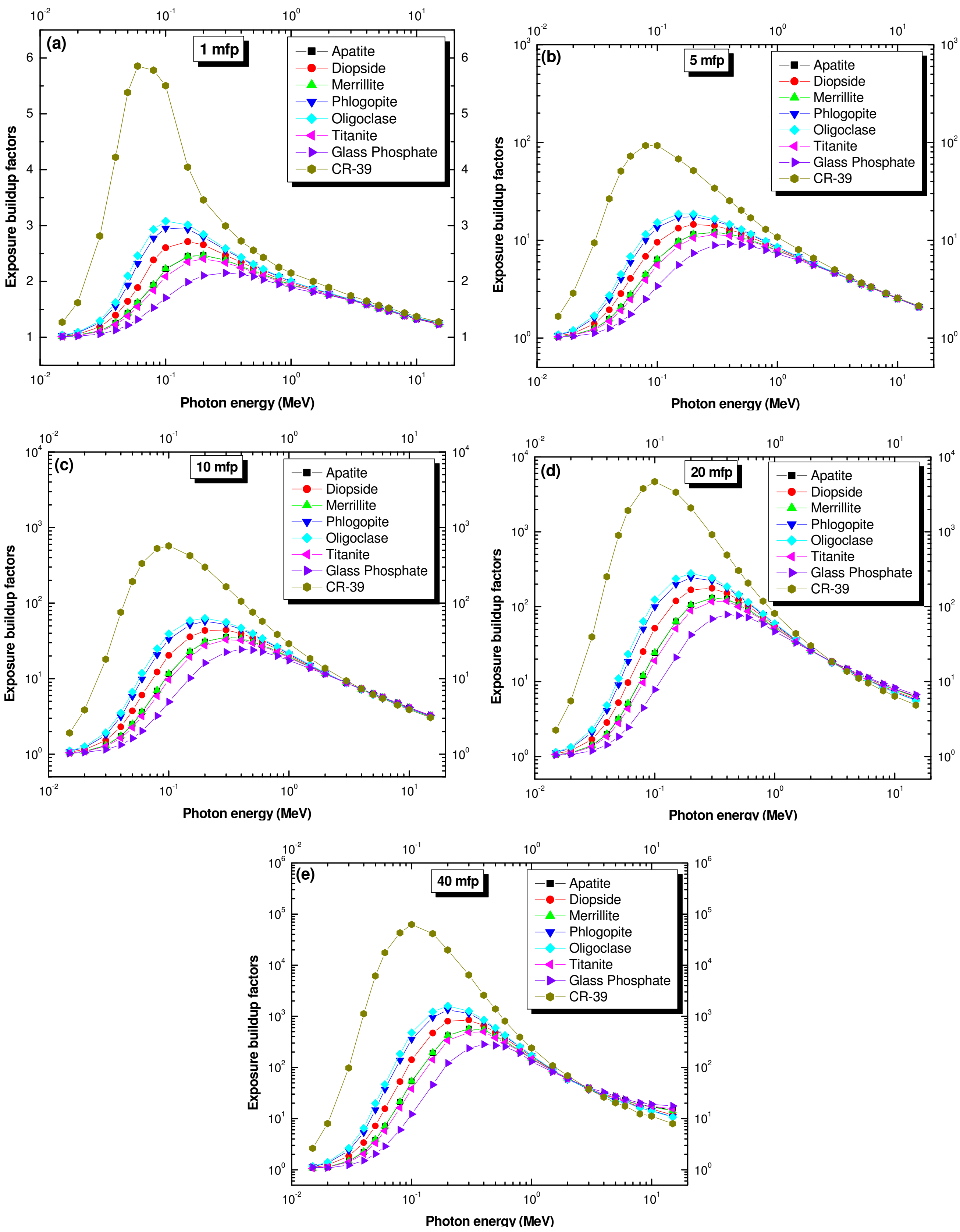

Fig. 3 — Exposure build-up factors of solid state neutron tract detectors (a) 1 mfp (b) 5 mfp (c) 10 mfp (d) 20 mfp and (e) 40 mfp penetration depths

4.1 Energy dependency of energy absorption buildup factors and exposure buildup factors

The variation of EABFs and EBFs of SSNTDs, apatite, diopside, merrillite, phlogopite, oligoclase, titanite, glass phosphate and CR-39 for photon energy in the range 0.015-15 MeV is shown in Figs 2 (a-e) and 3 (a-e). It was noted that the EABF and EBF values of the SSNTDs were minimum for low-and high-energy photon whereas these are the highest in the intermediate-energy. The build-up factors in low-energy were found to be small because the photons have completely been removed during the photo-electric absorption, gradually increase with the photon energy due to multiple scattering by Compton scattering in the intermediate-energy and finally reduce in high-energy region due to pair-production process. The $EABF_{max}$ of SSNTDs were found at energy 0.3, 0.2, 0.3, 0.2, 0.2, 0.4, 0.4 and 0.1 MeV for apatite, diopside, merrillite, phlogopite, oligoclase, titanite, glass phosphate and CR-39, respectively. The analysis shows that the highest EABFs and EBFs of the detector were found to be for CR-39 SSNTD in low-and intermediate photon energy region (<3 MeV). The pattern of build-up factors becomes reverse in high energy region (>3MeV).

4.2 Penetration depth dependency of energy absorption buildup factors and exposure build-up factors

The EABFs and EBFs of the selected SSNTDs increase with the penetration depths as shown for penetration depths 1, 5, 10, 20 and 40 mfp in Figs 2 (a-e) and 3 (a-e). It can be seen that the EABFs and EBFs of the glass phosphate are the lowest and highest for CR-39 in low penetration depth of range of 10 mfp. This can be explained by Z_{eq} of the SSNTDs at low photon energy, the low values of build-up factors are due to predominance of photo-electric effect which results in the complete removal of low energy photons thereby not allowing them to build-up in the medium. Thus, glass phosphate with highest Z_{eq} values show the lowest EABFs and EBFs.

The EABFs and EBFs of SSNTDs were found to be roughly constant (~ unity) at 0.015 MeV photon energy which increase with the penetration depth. It can be seen from Figs 2 (a-e) and 3 (a-e) that the values of EABF and EBF increase with increase in Z_{eq} at 15 MeV as penetration depth increases. The reason for reversal behaviour of such type of variation may be that beyond 3 MeV, the pair-production is dominant on the Compton scattering and produces the electron-positron pairs. These pair particles may escape from the detector medium of lower penetration depth whereas will multiple scatter in large penetration depths as well as start off the secondary gamma photons (0.511 MeV) by annihilation to increase the gamma photon intensities. Analysis signifies that the EABFs and EBF for CR-39 dosimeter are the minimum at large penetration depths (>10 mfp) in photon energy region above 3 MeV.

4.3 Chemical composition dependency of energy absorption buildup factors and exposure buildup factors

The build-up factors are dependent on the atomic number of elements hence EABF and EBF values of the SSNTDs were investigated for chemical compositions. Table 2 presents that the value of Z_{eq} of the SSNTDs increases slowly and become constant around photon energy ~1 MeV and afterwards starts reducing. The chemical composition dependency of the EABF and EBF values was analyzed for the photon energy at constant penetration depths. The reason for peaked EBF values is that the photo-electric and pair-production are dominant interaction processes in low and high-energy photon. respectively which completely remove the photons. The intermediate-energy photon take over Compton scattering where photon goes under multiple scattering events to build-up the photon. It is obvious that the SSNTDs are having large weight fraction of low-Z elements which are showing high EABF and EBF values due to less removal of the photons.

Moreover, it was observed that the EABF and EBF values among the SSNTDs, CR-39 showed maximum whereas glass phosphate showed minimum at particulate penetration depth below 3 MeV. The reason for it is that CR-39 is having lower Z_{eq} due to H (Z=1, w_f= 0.066), C(Z=6, w_f=0.525) and O(Z=8, w_f=0.408). However, glass phosphate is having high Z_{eq} due to O (Z=8, w_f=0.423), Na (Z=11, w_f=0.029), Al(Z=13, w_f= 0.026) and P(Z=15, w_f= 0.240) and Zn(Z=30, w_f= 0.281). the absence of low atomic number elements. It shows that the EABFs and EBFs of the SSNTDs decrease with increase in the Z_{eq} below penetration depth 10 mfp.

The EABF and EBF values of the SSNTDs increase with increase in Z_{eq} beyond 10 mfp and above photon energy of 3 MeV. It is due to the fact that photo-electric absorption cross-section is dependent on Z^{4-5}/E^{3-4} and pair-production cross-section is proportional to Z^2 therefore, pair-production is the dominant interaction process beyond 3 MeV. The pair-production will produce the electron-positron pairs which will scatter inside the detector materials. The positrons at rest annihilate with the electrons and generate 0.511 MeV secondary photons which increase the photon intensity in the medium and there EBF values increase in high penetration depths. The photon of 0.511 MeV energy is having high Compton cross-section which increase the EABF and EBF values by multiple scattering events before removal. We also noted that the EABF and EBF values for high-energy photon at large penetration depth are constant for high Z_{eq}. Thus. EABF and EBF values of the SSNTD materials are dependent on the chemical compositions.

5 Conclusions

The gamma ray build-up factors of solid state neutron track detectors (SSNTDs) were calculated by Geometrical Progression method in the energy range 0.015–15 MeV up to a penetration depth of 40 mean free paths. The results show that energy absorption and exposure build-up factors of build-up factors of SSNTDs are the highest in medium energy range whereas minimum in low and high photon energies. The maximum build-up factors exist for SSNTDs at 0.1 to 0.4 MeV for the detectors. The build-up factors for a fixed penetration depth are very large in the medium energy range and small in the low and high energy regions. The results show that for a fixed penetration depth the values of exposure build-up factor are very large in the medium energy range and small in the low and high energy regions. This study should be applicable for dosimetric purposes of the solid state neutron track detectors.

References

1 Shi-Lun G, Bao-Liu C & Durrani S A, Handbook of *Radioactivity Analysis* (III), Chapter 4 (2012).
2 Durrani S A & Bull R K, Pergamon Press, Oxford, (1987).
3 Kodaira S, Yasuda N, Konishi T, Kitamura H, Kurano M, Kawashima H, Uchihori Y, Ogura K & Benton E R, *Radia Meas*, 50 (2013) 232.
4 Forsley L P, Mosier-Boss P A, McDaniel P J & Gordon F E, *Electrochimica Acta,* 88 (2013) 373.
5 Cheol-Soo P, Jae-Hwan C, Hae-Kag L, Sun-Yeob L, Hyon-Chol J, Kyung-Rae D, Woon-Kwan C, Lee J, Deog-Hwan M, Kwang-Sung L, Nam-Oh Y & Moo-Seong C, *Ann Nuclear Ener*, 51 (2013) 196.
6 Khan N A, Khan H A, Gul K, Akbar R A, Anwar M, Waheed A, Hussain G & Shaikh M S, *Nucl Instrum Methods*, 173 (1980) 137.
7 Khan N A, Khan H A, Gul K, Anwar M, Hussain G, Akbar R A, Waheed A & Shaikh M S, *Nucl Instrum Methods*, 173 (1980) 163.
8 Wang T, Han H, Meng O, Wang L, Zhu L & Xia H, *Nucl Instru Meth Phys Res*, 697 (2013) 7.
9 Mayer S, Boschung M, Fiechtner A, Hohmann E, Fehrenbacher G, Radon T, Pleskac R & Wengenroth M, *Radia Meas*. 45 (2010) 1560.
10 Kaur R, Singh S, Singh K & Pandey O P, *Radia. Phys Chem*. 86 (2013) 23.
11 Ota S, Yasuda N, Sihver L, Kodaira S, Kurano M, Naka S, Ideguchi Y, Benton E R & Hasebe N, *Nucl Instru Meth Phys Res*, 269 (2011) 1382.
12 Milenković B, Nikezić D & Stevanović N, *Radia Meas*, 45 (2010) 1338.
13 Khan H A, *J Islamic Acad. Sci*, 3 (1990) 55.
14 Espinosa G, Golzarri J I, Chavarria A & Castaño V M, *Radia Meas*, 50 (2013) 127.
15 Rezaie M R, Sohrabi M, Negarestan A, Mohammadi S & Afzali D, *Radia Meas*, 50 (2013) 145.
16 Shang B, *Nucl Trac Radia Meas*, 22 (1993) 451.
17 Tommasino L & Espinosa G, *Radiat Meas*, 50 (2013) 22.
18 Lounis-Mokrani Z, Guittoum A, Imatoukene D, Aitziane M, Badreddine A & Mebhah M, *Radia Meas*, 50 (2013) 26.
19 Sahani P K, Haridas G & Sarkar P K, *Indian J Pure & Appl Phys*, 50 (2012) 863.
20 Fiechtner A & Wernli C, *Radiat Prot Dosimetry*, 85 (1999) 35.
21 Khan H A, Akbar R A, Hussain G, Hussain A & Jamil M, *Appl Radiat Isot*, 29 (1978) 49.
22 Kalsi P C, *Indian J Phys,* 83 (2009) 799.
23 Medhat M E, *Ann Nucl Ener*, 38 (2011) 1252.
24 Brahimi S, Lounis-Mokrani Z, Imatoukene D, Badreddine A, Abdelaziz F Z & Allab M, *Radia Meas*. 43 (2008) 56.
25 Singh S Neerja, *Radia Meas*, 42 (2007) 1507.
26 ANSI/ANS-6.4.3, Gamma ray attenuation coefficient and buildup factors for engineering materials, (1991).
27 Shimizu A, Onda T & Sakamoto Y, *Nucl Sci Technol*, 41 (2004) 143.
28 Harima Y, Sakamoto Y, Tanka S & Kawai M, *Nucl Sci Engg*, 94 (1986) 24.
29 Harima Y, *Radiat Phys Chem*, 41(4/5) (1993) 631.
30 Mann K S & Korkut T, *Ann Nucl Ener*, 51 (2013) 81.
31 Kurudirek M, Sardari D, Khaledi N, Çakır C & Mann K S, *Ann Nucl Ener*, 53 (2013) 485.
32 Singh V P & Badiger N M, *Int J Nucl Ener Sci Tech*, 7 (1) (2012) 75.
33 Kurudirek M & Topcuoglu S, *Nucl Instru Meth Phys Res*, 269 (2011) 1071.
34 Manohara S R, Hanagodimath S M & Gerward L, *Radia Phys Chem*, 79 (2010) 575.
35 Kucuk N, Manohara S R, Hanagodimath S M & Gerward L, *Radia Phys Chem*, 86 (2013) 10.
36 Gerward L, Guilbert N, Jensen K B & Levring H. *Radi Phys Chem*, 60 (2001) 23.
37 Gerward L, Guilbert N, Jensen K B & Levring H, *Radi Phys Chem*, 71 (2004) 653.
38 Berger M J, Hubbell J H, Seltzer S M, Chang J, Coursey J S, Sukumar R, Zucker D S & Olsen K, (2010). XCOM: photon cross sections database, NIST standard reference database (XGAM).http://www.nist.gov/pml/data/xcom/index.cfm.
39 Maron M J, Numerical analysis: A Practical approach, Macmillan, New York, 2007.
40 Harima Y, *Nucl Sci Engg*, 83 (1983) 299.
41 Luis D, (2009) Update to ANSI/ANS-6.4.3-1991 for low-Z materials and compound materials and review of particle transport theory, UNLV, Las Vegas, NV 89154.
42 Berger M J, Naval Radiological Defence Laboratory, USNRDL Review and Lectures No. 29 (1956) 47.
43 Taylor J J, (1954) Application of gamma ray buildup data to shield design, WAPD-RM-217.
44 Foderaro A & Hall R J, *Nucl Sci Engrg*. 78 (1981) 74.